Legume receptors perceive the rhizobial lipochitin oligosaccharide signal molecules by direct binding

Angelique Broghammer[a,b], Lene Krusell[a,b], Mickaël Blaise[a,b], Jørgen Sauer[a,c], John T. Sullivan[a,d], Nicolai Maolanon[a,c], Maria Vinther[a,b], Andrea Lorentzen[e], Esben B. Madsen[a,b], Knud J. Jensen[a,c], Peter Roepstorff[e], Søren Thirup[a,b], Clive W. Ronson[a,d], Mikkel B. Thygesen[a,c], and Jens Stougaard[a,b,1]

[a]Centre for Carbohydrate Recognition and Signalling, [b]Department of Molecular Biology and Genetics, Aarhus University, DK-8000 Aarhus, Denmark; [c]Department of Chemistry, Faculty of Science, University of Copenhagen, DK-1871 Frederiksberg C, Denmark; [d]Department of Microbiology and Immunology, University of Otago, Dunedin 9054, New Zealand; and [e]Department of Biochemistry and Molecular Biology, University of Southern Denmark, DK-5230 Odense M, Denmark

Edited by Jeffery L. Dangl, University of North Carolina, Chapel Hill, NC, and approved July 4, 2012 (received for review March 28, 2012)

Lipochitin oligosaccharides called Nod factors function as primary rhizobial signal molecules triggering legumes to develop new plant organs: root nodules that host the bacteria as nitrogen-fixing bacteroids. Here, we show that the *Lotus japonicus* Nod factor receptor 5 (NFR5) and Nod factor receptor 1 (NFR1) bind Nod factor directly at high-affinity binding sites. Both receptor proteins were posttranslationally processed when expressed as fusion proteins and extracted from purified membrane fractions of *Nicotiana benthamiana* or *Arabidopsis thaliana*. The N-terminal signal peptides were cleaved, and NFR1 protein retained its in vitro kinase activity. Processing of NFR5 protein was characterized by determining the *N*-glycosylation patterns of the ectodomain. Two different glycan structures with identical composition, $Man_3XylFucGlcNAc_4$, were identified by mass spectrometry and located at amino acid positions N68 and N198. Receptor–ligand interaction was measured by using ligands that were labeled or immobilized by application of chemoselective chemistry at the anomeric center. High-affinity ligand binding was demonstrated with both solid-phase and free solution techniques. The K_d values obtained for Nod factor binding were in the nanomolar range and comparable to the concentration range sufficient for biological activity. Structure-dependent ligand specificity was shown by using chitin oligosaccharides. Taken together, our results suggest that ligand recognition through direct ligand binding is a key step in the receptor-mediated activation mechanism leading to root nodule development in legumes.

lysin motif proteins | plant–microbe interactions | symbiotic signalling | lysin motif receptor-like kinase | non-self recognition

Formation of nitrogen-fixing root nodules relies on an intriguing signal exchange between the legume host and the bacterial microsymbiont (1). In this two-way exchange, Nod factors synthesized by rhizobia function as central signal molecules, which induce early physiological responses, gene expression, and cell division in susceptible legumes (1–3). In root cells of the legume hosts, perception is mediated by Nod factor receptors (NFRs) containing ectodomains with three lysin motif (LysM) modules and cytoplasmic serine/threonine kinase domains (4–9). Mutant studies in the model legumes *Lotus japonicus* (*Lotus*) and *Medicago truncatula* (*Medicago*) as well as the crop legumes soybean (10, 11) and pea (5, 6) have shown that NFRs are required for nodulation. Mutant analysis in *Lotus* identified two NFRs, NFR1 and NFR5, and phenotypic analysis showed that both *nfr1* and *nfr5* mutants are equally impaired in nodule initiation (4, 5). In *Medicago*, only mutation of the *Nfr5* ortholog, *Nfp,* results in a nonnodulating phenotype, whereas the *Nfr1* homolog *Lyk3* is required for progression of infection threads (7–9, 12).

The earliest plant responses to Nod factor, such as membrane depolarization, cytoplasmic alkalinization, calcium fluxes, calcium spiking, and root hair deformation (3, 13), are either strongly attenuated or absent in the *Lotus nfr1* and *nfr5* mutants and the *Medicago nfp* mutant (4, 5, 7–9). In wild-type plants, these responses are induced by Nod factor concentrations in the nano- to picomolar range (14–16). Experiments pursuing the subsequent receptor activation process have shown kinase activity from both the *Lotus* NFR1 and the *Medicago* LYK3 cytoplasmic domains expressed in *E. coli*. Several autophosphorylation sites were detected in their kinase domains and intermolecular autophosphorylation with dual specificity for Ser/Thr and Tyr was observed (17, 18). Using the same assay, kinase activity was not detected for the cytoplasmic domains of NFR5 and NFP. However, NFR1 transphosphorylated NFR5 at a single Ser residue (17). So far, all of the NFRs from different legumes are predicted to have a single transmembrane domain. Membrane localization of *Lotus* NFR1 and NFR5 was shown in *Nicotiana benthamiana* leaf cells and by copurification of the expressed proteins with the plasma membrane (17). In *Medicago* LYK3-GFP fusion proteins were associated with puncta located in the plasma membrane or in membrane-tethered vesicles (19), whereas NFP localized to the plasma membrane in *N. benthamiana* (20). Further insight into the NFR receptor-mediated signaling came from assays of protein-complex formation by using a split YFP system and confocal microscopy in *N. benthamiana* leaf cells (17). Interaction between membrane-bound NFR1 and NFR5 detected as bimolecular fluorescence complementation was observed only when a kinase-inactive NFR1 was expressed together with NFR5. In contrast, a rapid NFR5-dependent cell death response was observed after expression of a kinase-active NFR1 (17). A heterocomplex of NFR1 and NFR5 was thus capable of initiating a signal transduction process.

Genetic analysis in *Lotus* has placed NFR1 and NFR5 activation upstream of two signal transduction pathways leading to infection thread formation and root nodule organogenesis, respectively (21). The simplest interpretation supports a mechanism in which Nod factor perception by a NFR complex (17) at the plasma membrane leads to activation of the NFR1 kinase. This activation, in turn, triggers downstream signal transduction through phosphorylation. In agreement with this mechanism, domain swap experiments and amino acid substitution studies have demonstrated that the ectodomains of the NFR5 and NFP receptors mediate Nod factor perception and that single amino acid variations in the LysM2 module change recognition of Nod factor variants (22, 23). Allelic variation in the pea *SYM37* gene, leading to amino acid differences

Author contributions: A.B., L.K., K.J.J., M.B.T., and J. Stougaard designed research; A.B., L.K., M.B., J. Sauer, J.T.S., N.M., M.V., A.L., E.B.M., and M.B.T. performed research; A.B., L.K., M.B., J. Sauer, J.T.S., N.M., A.L., P.R., S.T., C.W.R., M.B.T., and J. Stougaard analyzed data; and A.B. and J. Stougaard wrote the paper.

The authors declare no conflict of interest.

This article is a PNAS Direct Submission.

Freely available online through the PNAS open access option.

[1]To whom correspondence should be addressed. E-mail: stougaard@mb.au.dk.

This article contains supporting information online at www.pnas.org/lookup/suppl/doi:10.1073/pnas.1205171109/-/DCSupplemental.

in the LysM module of the encoded protein, was similarly suggested to account for differences in pea nodulation (6, 24). However, direct receptor binding of the Nod factor demonstrating a receptor–ligand relationship has not been shown and progress has been hampered by the recalcitrant biochemical properties characteristic of single-pass membrane proteins and by the amphiphilic nature of Nod factors.

We have investigated the in vitro ligand binding capacity of the *Lotus* NFR5 and NFR1 receptor proteins. Methods for expression of full-length proteins were established, and two different techniques were used for characterizing receptor–ligand interactions and determining K_d values for Nod factor binding.

Results

Expression and Purification of NFR1 and NFR5 Fusion Proteins. Attempts to express NFR proteins in *Escherichia coli*, yeast, or mammalian cells were largely unsuccessful, producing low yields and aggregated proteins. Plant-based expression systems were also explored because they appeared to be more suitable for processing and compartmentalization of plant membrane proteins. Expression of NFR1 and NFR5 was accomplished by transient expression in *N. benthamiana* and by stable expression of NFR5 in *Arabidopsis thaliana*. Optimal transient expression was achieved by infiltration of leaves of 3-wk-old greenhouse-grown *N. benthamiana* plants by using *Agrobacterium tumefaciens* AGL1. Because expression levels between experiments were variable, and protein yield had to be balanced against cellular aggregation, full-length NFR1 and NFR5 were expressed as GFP/YFP fusion proteins that could be monitored by using confocal microscopy. Confocal microscopy was also used to identify primary *A. thaliana* transformants expressing NFR5-YFP fusion protein before further propagation and seed multiplication. We were unable to establish stable lines expressing NFR1.

For extraction of NFR1 and NFR5 proteins, plasma membranes were isolated and purified by aqueous two-phase partitioning. To release the proteins from the membrane fraction, 21 detergents were tested. Apart from SDS, only Fos-Choline 10 and *n*-decyl-α-D-maltopyranoside solubilized the two proteins, and Fos-Choline 10 was chosen for further work. The purification protocol involved isolation of plasma membranes or microsomal membranes by two-phase partitioning and differential centrifugation, protein solubilization from the plasma membrane or the microsomal fraction, affinity purification (Fig. 1*A*), gelfiltration (Fig. 1 *B* and *C*), and finally protein quantification by in-gel fluorescence (Fig. 1*B*) with a recombinant GFP standard. Approximately 25 μg of full-length NFR1 or NFR5 protein was extracted from 1 kg of plant material by using this procedure (Fig. 1*B*). Starting from the microsomal fraction, a 40-fold enrichment was observed in the final gelfiltration-purified protein samples as determined by using in-gel fluorescence.

Processing and Activity of the NFR Proteins. Bioinformatic analysis predicted that the NFR proteins would be synthesized with an N-terminal signal peptide for entry to the endoplasmic reticulum and the secretory pathway, where posttranslational modification occurs. To assess the entry into the secretory pathway in the heterologous expression systems, the N-termini of purified NFR1 and NFR5 proteins were sequenced. For NFR5, the N-terminal sequence confirmed processing of the predicted 26-aa signal peptide (5) (Fig. S1*A*). However, the original prediction for NFR1 was less precise. Instead of the predicted 17 amino acids (4), sequencing identified a signal peptide of 23 or 24 amino acids, which is consistent with predictions achieved by using SignalP version 4.0 (Fig. S1*B*). This N-terminal processing removed one cysteine from the mature protein, leaving six cysteines arranged in three pairs in the processed ectodomain, as for NFR5 (Fig. S1 *A* and *B*).

Kinase activity was used to verify functionality of the full-length NFR1-GFP fusion protein purified from *N. benthamiana.* Both autophosphorylation and phosphorylation of Myelin basic protein (MyBP) was observed for the full-length NFR1-GFP protein (Fig. 1 *D* and *E*), confirming results obtained with the kinase domain expressed in *E. coli*. In contrast, no kinase activity was detected from the NFR5-GFP full-length protein, consistent with the absence of detectable kinase activity from the NFR5 kinase domain expressed in *E. coli* (Fig. 1*E*).

Because N-glycosylation is a common posttranslational modification of plasma membrane-localized proteins, glycosylation of NFR5 was assessed as a measure of processing. N-glycosylation of NFR5 at the five possible N-glycosylation motifs NXS/T (X ≠ P, D) in its ectodomain (Fig. S1*A*) was determined by using MALDI TOF/TOF mass spectrometry. Protein bands containing NFR5 expressed in *N. benthamiana* or *A. thaliana* were excised

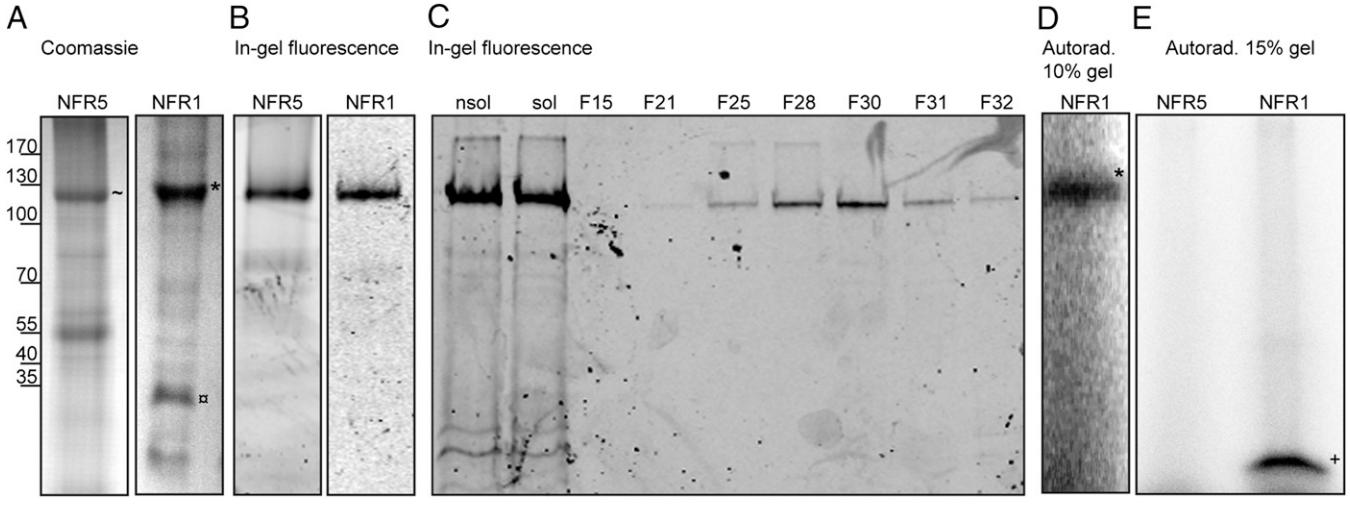

Fig. 1. Protein purification and NFR1 kinase assay. (*A*) Coomassie gel of NFR1-GFP and NFR5-GFP, respectively, after affinity purification. ~, NFR5; *, NFR1; ¤, YFP degradation product. (*B*) In-gel fluorescence of NFR1-GFP and NFR5-GFP, respectively, after gelfiltration. (*C*) In-gel fluorescence of NFR5-YFP fractions after gelfiltration purification. F, fraction; nsol, nonsolubilized plasma membrane fraction; sol, solubilized plasma membrane fraction. (*D* and *E*) In vitro kinase assay with recombinant NFR5 and NFR1. (*E*) NFR5 shows no kinase activity. +, MyBP. (*D* and *E*) NFR1 shows cross-phosphorylation of MyBP and autophosphorylation.

from SDS/PAGE gels. N-glycosylation was detected by comparing MS spectra of glycosylated and deglycosylated peptides obtained after digestion with three different enzymes followed by enrichment of glycosylated peptides by chromatography (Fig. S2). Subsequent fragmentation (MS/MS) of the relevant ion species identified two glycan structures with identical sugar composition ($Man_3XylFucGlcNAc_4$), which were linked to N68 and N198 of NFR5 (Table 1 and Table S1). Additional mannose-rich glycans were identified at N68 and N198 of the NFR5 protein purified from *N. benthamiana* microsomal fractions. These glycan structures most likely reflect ongoing processing in the transient expression system (Table S1). Importantly, glycan structures containing glucose, indicative of aberrant processing, were not detected. In addition, the 35S-NFR5-GFP construct used for protein expression complemented the *Lotus nfr5-2* mutant giving 4.4 nodules per plant ($n = 50$), a result similar to that previously found for the wild-type *Nfr5* gene (5), indicating that the NFR5-GFP fusion protein was functional *in planta*.

NFR1 and NFR5 Receptor Proteins Bind Nod Factor Directly. The physical interaction between Nod factor and NFR1 or NFR5 was initially visualized in a bead-based assay. GFP-tagged NFR1 or NFR5 protein (30 nM) were immobilized on the surface of GFP-Trap agarose beads (25), washed, and inspected by confocal microscopy. Binding of GFP-fusion proteins to beads resulted in strong green fluorescence (Fig. 2*A*). Nod factor isolated from *M. loti* was chemoselectively functionalized through the reducing end by aniline-catalyzed oxime formation (26, 27). This functionalization allowed the introduction of a PEG spacer with a thiol group, which was reacted with the $Alexa_{546}$ fluorophore (Figs. S3*A* and S4*E*). Incubation of beads with immobilized protein and 10^{-6} M Nod factor resulted in strong green fluorescence from GFP and red fluorescence from $Alexa_{546}$ (Fig. 2*A* and Fig. S5*A*). Application of four NFR1-GFP or NFR5-GFP concentrations (10, 5, 2, and 1 nM) followed by incubation with 10^{-6} M $Alexa_{546}$-labeled Nod factor showed protein-dependent ligand binding (Fig. 2*C* and Fig. S5*B*). To validate the bead-based Nod factor binding assay, a series of control experiments were carried out. In summary, they showed (*i*) absence of $Alexa_{546}$ Nod factor binding to GFP-Trap agarose beads (Fig. S6*A*); (*ii*) absence of $Alexa_{546}$ Nod-factor binding to immobilized GFP (Fig. S6*B*); (*iii*) no NFR1 or NFR5 binding of the fluorophore label or PEG linker (Fig. S4*A*) used for coupling of the fluorescent dye to Nod factor (Fig. S6*D*); (*iv*) no nonspecific fluorescence background in microsomal membrane preparations (Fig. S6*C*); and (*v*) biological activity of $Alexa_{546}$-labeled Nod factor (Fig. S8).

The ligand specificity of NFR1 and NFR5 was tested with a set of chitin oligomers $(GlcNAc)_x$. Addition of 10^{-6} M $Alexa_{546}$-labeled $(GlcNAc)_2$, $(GlcNAc)_3$, or $(GlcNAc)_5$ (Fig. S4*B*) to NFR5-GFP or NFR1-GFP beads resulted in barely detectable red fluorescent signals (Fig. 2*B* and Fig. S5*A*), whereas the signal from 10^{-5} M $Alexa_{546}$-labeled $(GlcNAc)_2$, $(GlcNAc)_3$, or $(GlcNAc)_5$ was comparable with the fluorescence intensity observed to 10^{-6} M $Alexa_{546}$-labeled Nod factor.

In competition experiments, excess unlabeled Nod factor added before $Alexa_{546}$-labeled Nod factor diminished the red fluorescence below detection (Fig. 2*D* and Fig. S5*C*). A slight difference in Nod factor binding was observed, when excess unlabeled chitin oligomers $(GlcNAc)_x$ were added before labeled Nod factor (Fig. 2*D*). However, the red fluorescence intensities observed in the Nod factor and $(GlcNAc)_x$ competition experiments indicate a lower affinity for $(GlcNAc)_x$ than for Nod factor, which was able to completely out-compete binding of labeled Nod factor.

NFR1 and NFR5 Receptor Proteins Bind Nod Factor with High Affinity. The GFP-bead binding assay is a visually attractive method for demonstrating direct physical interactions. However, quantification of fluorescence intensities using the confocal microscope (Fig. S7) was laborious and the sensitivity was inadequate for work with the nano- to picomolar concentrations of Nod factor that are sufficient for biological activity. Binding affinity was therefore investigated by using surface plasmon resonance (SPR) on a Biacore T100 instrument. We took advantage of recently developed carbohydrate-linker chemistry (26) to immobilize oxime glycoconjugates of Nod factor, $(GlcNAc)_5$, and glucose by thiol coupling on a sensor chip (Fig. S3*B*). To determine binding affinities with the Nod factor receptors, the following ligands were reacted onto three flow cells (Fc) of a CM5 sensor surface: Fc1, glucose-conjugate as reference (Fig. S4*C*); Fc2, $(GlcNAc)_5$-conjugate (Fig. S4*D*); Fc3, Nod factor-conjugate (Figs. S3*B* and S4*E*). Wheat germ agglutinin (WGA), a lectin with a known affinity toward GlcNAc, was used as a control to validate the sensor chip analysis. The sensorgrams obtained for WGA addition to $(GlcNAc)_5$ and Nod factor, in Fc2 and 3, respectively, showed a time-dependent response with rapid association and dissociation (Fig. S8 *C* and *D*). No obvious difference between WGA binding to $(GlcNAc)_5$ compared with Nod factor was detected (Fig. 3*A* and Fig. S8 *C* and *D*). The dissociation constants were determined by analyzing the equilibrium response versus protein concentration using a nonlinear fit (GraphPad Prism 5). K_d values of 15 ± 3 μM and 25 ± 8 μM were found for Nod factor and $(GlcNAc)_5$, respectively (Table 2). These binding constants are in the same range as the K_d of 47 μM, which was determined by passing $(GlcNAc)_5$ over a sensor chip with immobilized WGA (28).

When purified NFR1-GFP or NFR5-GFP protein (Fig. 1 *A* and *B*) was added to the sensor chip, clear association and dissociation phases were observed in the sensorgram of Fc3 containing

Table 1. List of complex N-glycan structures found on NFR5 protein expressed in *A. thaliana* and *N. benthamiana*, respectively

ES	Enzyme	Peptide sequence of glycosylated peptide after digestion	*m/z*	N-glycan structures
At	Asp-N	DN(198)VSLVSAKFGASPA	3039	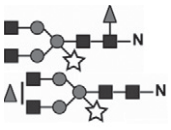
At	Trypsin	GIQYLITYVWKPNDN(198)VSLVSAK	4085	
Nb	Asp-N	DN(198)VSLVSAKFGASPA	3039	
At	Chymotrypsin	RSEKISGPDFSCPVDSPPSCETYVTYTAQSPNLLSLTN(68)ISDIFDISPL	6895*	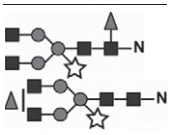
Nb	Asp-N	RSEKISGPDFSCPVDSPPSCETYVTYTAQSPNLLSLTN(68)IS	5994*	
Nb	Chymotrypsin	RSEKISGPDFSCPVDSPPSCETYVTYTAQSPNLLSLTN(68)ISDIFDISPL	6896	

At, *A. thaliana*; ES, expression system; *Nb*, *N. benthamiana*; ▲, fucose; ●, mannose; ■, *N*-acetylglucosamine; ☆, xylose.

*The peptide sequence was verified with MS/MS.

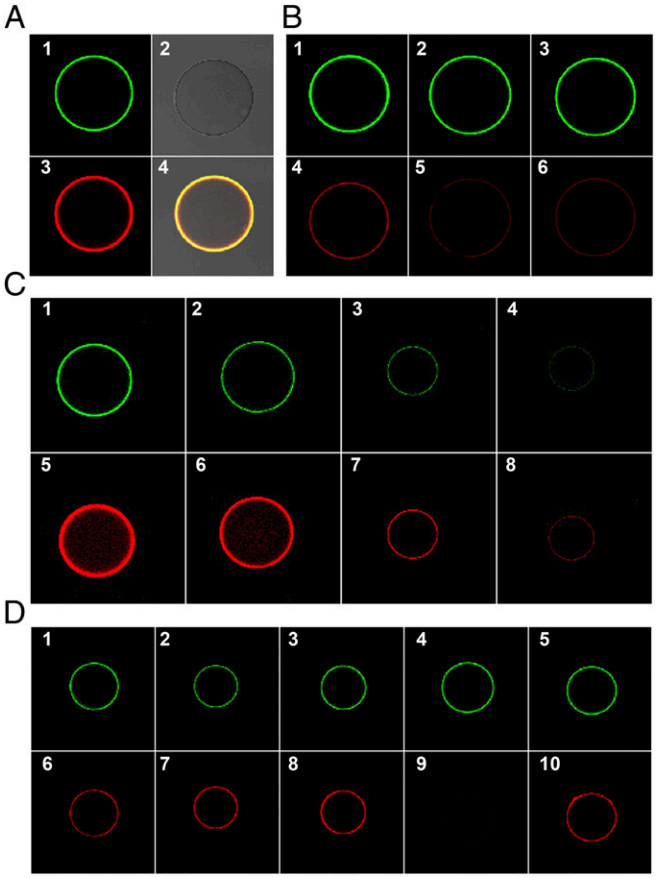

Fig. 2. NFR5 binds Nod factor and GlcNAc oligomers in the bead assay. (*A*) Interaction of NFR5 with Nod factor. (*A1*) Fluorescence of NFR5-GFP (30 nM) bound to GFP nanotrap beads. (*A2*) Bright field picture of a GFP nanotrap bead. (*A3*) Fluorescence of 10^{-6} M $Alexa_{546}$-labeled Nod factor bound by the NFR5 protein. (*A4*) Overlay of *A1–A3*. (*B*) Interaction of NFR5 with $(GlcNAc)_x$ oligomers: (*B1–B3*) Fluorescence of NFR5-GFP (30 nM) beads. (*B4–B6*) Fluorescence of 10^{-6} M $Alexa_{546}$ labeled $(GlcNAc)_2$, $(GlcNAc)_3$, and $(GlcNAc)_5$, respectively, bound by the NFR5 protein. (*C*) Interaction of NFR5 with Nod factor is concentration dependent: (*C1–C4*) Green fluorescence of 10, 5, 2, and 1 nM NFR5-GFP protein beads. (*C5–C8*) Red fluorescence of 10^{-6} M $Alexa_{546}$ labeled Nod factor bound by the NFR5 protein shown in *C1–C4*, respectively. (*D*) Competition experiments. (*D1–D5*) Fluorescence of the 10 nM NFR5-GFP protein beads. (*D6–D10*) Corresponding fluorescence of 10^{-6} M $Alexa_{546}$-labeled Nod factor bound by NFR5 after previous incubation with 10^{-4} M unlabeled $(GlcNAc)_2$ (*D6*), $(GlcNAc)_3$ (*D7*), $(GlcNAc)_5$ (*D8*), *M. loti* Nod factor (*D9*), and buffer B (*D10*).

Nod factor (Fig. S9*A*). No time-dependent response could be measured with the reference surface of glucose in Fc1, which displayed only the increased refractive index from the injected NFR-GFP fusion protein. The dissociation constant was determined by analyzing the equilibrium response versus protein concentration using a nonlinear fit. Three independent protein preparations of NFR1 or NFR5 were tested and showed the same high-affinity binding toward Nod factor. The respective K_d values were 10.1 ± 2.5 nM for NFR5, 4.9 ± 1.3 nM for NFR1, and saturation was at ∼130 nM and 64 nM, respectively (Fig. 3*A*, Fig. S9*A*, and Table 2). In contrast, binding to $(GlcNAc)_5$ in Fc2 was not detected. Finally, GFP purified from *N. benthamiana* was used as a control on the chip and no binding was detected.

To further characterize the binding between the receptors and Nod factor, we used microscale thermophoresis (MST), an optical method that relies on the change of the hydration shell of biomolecules due to changes in their structural conformation upon binding of a ligand/interaction partner (29–31). These changes result in a relative mobility change of the protein in the applied temperature gradient and are used to determine binding affinities in free solution. Binding of large proteins to small ligands is expected to result in larger mobility shifts compared with the reverse experiment. Based on that assumption, we titrated NFR receptor proteins (∼100 kDa) to a constant concentration of $Alexa_{546}$-labeled Nod factor (∼1.5 kDa). Binding of NFR5 and NFR1 to Nod factor in the nanomolar range was observed (Fig. 3*B* and Fig. S9*B*). A change in the fluorescent signal was detected in the temperature jump for measurements with NFR5 and in the thermophoresis phase for measurements with NFR1. In contrast, no change in fluorescence signal was detected with labeled $(GlcNAc)_5$, labeled linker molecule nor for labeled Nod factor in the absence of the receptor proteins (Fig. 3*B*). The K_d values obtained for the interaction of NFR5 or NFR1 and labeled Nod factor were 4.0 ± 1.5 nM and 0.61 ± 0.25 nM, respectively (Table 2).

Discussion

We have established procedures for transient and stable expression of integral membrane Nod factor receptor proteins. The *Lotus* NFR1 and NFR5 receptors were purified as YFP or GFP fusion proteins from membranes of *A. thaliana* and/or *N. benthamiana* in amounts sufficient for determination of ligand-binding affinities of these recalcitrant proteins. Attempts to establish stable NFR1 expression in *A. thaliana* failed. We assume that a high level of NFR1 protein induces downstream signaling leading to cell ablation. Supporting this notion, cell death, comparable to that observed after low-level expression of NFR1 together with NFR5 (17), was observed during attempts to express NFR1 at high levels in *N. benthamiana*. High-level expression of NFR5 did not induce this cell death response, and NFR5 appears to completely depend on complex formation with the kinase-active NFR1 protein to play its role in signal initiation. Together, these observations corroborate our in vitro results showing kinase activity of purified NFR1 and also strengthen the conclusion that the NFR1 protein used for binding studies was folded and functional. Similar to NFR1 in *A. thaliana*, stable transgenic lines overexpressing LYK3 could not be obtained in *Medicago* (32).

Sequencing of the NFR1 and NFR5 N-termini showed that both receptor proteins were processed. For the NFR1 ectodomain, the experimentally determined N-terminal cleavage removed a cysteine originally predicted to be retained. Both NFR1 and NFR5 have six cysteines arranged in three pairs in their processed ectodomains and disulfide bridges between them probably affect the structure of the ectodomains as recently shown for CERK1 (33). Highlighting the importance of these cysteine pairs, amino acid substitutions in the corresponding cysteines of the NFP protein were shown to be functionally significant in complementation studies (34). Detailed analysis of the N-glycan structure of NFR5 by tandem mass spectrometry revealed two complex structures with identical sugar compositions ($Man_3XylFucGlcNAc_4$) at N68 and N198. Additionally, mannose-rich structures were found at N68 and N198 of NFR5 from microsomal fractions of *N. benthamiana*. This result suggests that processing was ongoing at the time of harvest and that the high-mannose proteins were extracted from the Golgi apparatus, because processing of glucose and some mannose moieties from $Glc_3Man_9GlcNAc_2$ precursors had occurred (35, 36). No reglucosylation after "quality control" processes in the endoplasmic reticulum (37) was detected, and we infer that NFR5 protein was folded and transferred to the Golgi apparatus. Two complex glycans ($Man_3XylFucGlcNAc_4$) and ($Man_3XylFuc_3Gal_2GlcNAc_4$) are predominantly found in extracellular proteins (35). The two structures ($Man_3XylGlcNAc_4$ and $Man_3GlcNAc_4$) found in the N-glycan analysis of NFR5 could thus be precursors. Glycosylation was also detected in the NFP protein from transgenic *Medicago* by polyacrylamide gel analysis (38). Together with our detailed MS analysis of glycan structures,

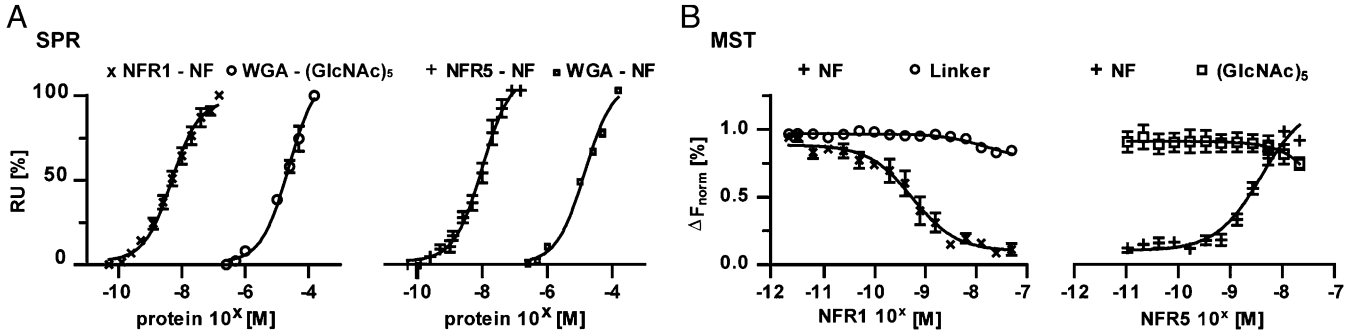

Fig. 3. NFR1 and NFR5 bind Nod factor in the nanomolar range. (*A*) Binding of WGA, NFR1, and NFR5 to immobilized $(GlcNAc)_5$ or Nod factor using SPR. Measurements were repeated with at least three independent protein preparations. The binding curves were obtained from the equilibrium response (R_{Eq}) by using a nonlinear fit (least squares fit). Error bars indicate the 95% confidence interval. WGA was applied at concentrations of 0.25–150 μM. (WGA-$GlcNAc)_5$: K_d = 25 ± 8 μM, R^2 = 0.98; (WGA-Nod factor): K_d = 15 ± 3 μM, R^2 = 0.99. NFR1 and NFR5 were applied at concentrations of 0.05–150 nM. (NFR1-Nod factor): K_d = 4.9 ± 1.3 nM, R^2 = 0.96; (NFR5-Nod factor): K_d = 10.1 ± 2.5 nM, R^2 = 0.94. (*B*) NFR1 and NFR5 bind to $Alexa_{546}$-labeled Nod factor, but not to labeled $(GlcNAc)_5$ or linker in MST experiments. The data were analyzed by plotting the protein concentration against the percent changes of normalized fluorescence (ΔF_{norm} [%]) of thermophoresis using a nonlinear fit (least squares fit). Error bars indicate the 95% confidence interval. (NFR1–Nod factor): K_d = 0.61 ± 0.25 nM, R^2 = 0.82; (NFR5–Nod factor): K_d = 4.0 ± 1.5 nM, R^2 = 0.91.

this observation indicates that NFRs have highly N-glycosylated ectodomains although a functional role could not be assigned in complementation studies using NFP (34). Overall our N-glycan analysis of NFR5 indicates that the NFR5 protein is folded and processed in both expression systems. Because N-glycan biosynthesis appears to be conserved in higher plants (36), we expect the ($Man_3XylFucGlcNAc_4$) N-glycan structure reflects the native structure in *Lotus*.

The *M. loti* Nod factor is composed of a pentameric GlcNAc backbone, which carries acetyl-fucose, carbamoyl, N-methyl, and $C_{18:1}$ N-acyl attachments (39, 40). Fully decorated Nod factor and chitin oligomer backbones were attached to an SPR sensor surface or linked to fluorophores at the reducing moiety by using chemoselective oxime chemistry and biological activity at 10^{-7} M was shown for fluorophore-labeled Nod factor (Fig. S8). The NFR1 and NFR5 receptor proteins bound these modified lipochitin oligosaccharides with K_d values in the nanomolar range. Although the bead assay detected $(GlcNAc)_5$ binding in the 10^{-5} to 10^{-6} M range, no high affinity binding of $(GlcNAc)_5$ was detected by using surface plasmon resonance or thermophoresis. An affinity comparable to the chitin-binding site of the CERK1 receptor, which is estimated to have a K_d of ~82 nM (41), was thus not detected in these assays. However, similar to CERK1 where binding of chitin beads required the presence of all three LysM modules (42), only one binding affinity was found.

Interestingly, the K_d values for NFR1 and NFR5 ligand binding are comparable to the 10^{-7} to 10^{-10} M Nod factor concentrations found to induce membrane depolarization, calcium influx, and calcium spiking in *Lotus* (4, 15). Experiments directly comparing chitin oligosaccharides and Nod factor effects in *Medicago* found that 10^{-9} M to 10^{-12} M of fully decorated Nod factor was sufficient to induce calcium spiking, whereas $(GlcNAc)_4$ at 10^{-4} M to 10^{-6} M was required for induction of calcium spiking (14). In pea root hairs, calcium spiking was induced by 10^{-8} M of Nod factor, whereas 10^{-6} M $(GlcNAc)_4$ or $(GlcNAc)_5$ was required to induce regular spiking (16). Considering these concentrations, the K_d values determined for NFR1 and NFR5 correspond to a high-affinity Nod factor-binding site required for biological activity. The similar ligand affinities of NFR1 and NFR5 are intriguing considering the NFR5 dependence on NFR1 kinase activity for downstream signaling. A mechanism whereby Nod factor binding at both receptor ectodomains promotes complex formation with the cytoplasmic domain of NFR5 being required for subsequent interaction with cellular factor(s) might explain this observation as well as the conservation of the NFR5 cytoplasmic domain. Recent structural analysis of the CERK1 ectodomain defined a single site in the LysM2 domain that binds chitin in the micromolar range (33), with $(GlcNAc)_8$ inducing receptor dimerization that was inhibited by $(GlcNAc)_5$. The suggested function of chitin as a bivalent ligand assembling CERK1 into functional dimers might exemplify such a mechanism, separating binding and receptor activity (33). *In planta* binding studies and binding studies on membrane fractions from *Lotus* root hairs of wild-type and *nfr1 nfr5* mutant plants could, in principle, provide additional insight into the NFR receptor mechanism in a cellular context. However, the low abundance of NFR receptor proteins and the "sticky" amphiphilic nature of the Nod factor make such approaches technically very challenging and separation of receptor-binding from membrane- or cell wall-binding difficult.

Table 2. Dissociation constants for binding of NFR5, NFR1, WGA, and GFP to $(GlcNAc)_5$ and Nod factor, respectively, determined by SPR and MST

	SPR		MST		
Protein	$(GlcNAc)_5$	Nod factor	Linker $Alexa_{546}$	$(GlcNAc)_5$ $Alexa_{546}$	Nod factor $Alexa_{546}$
NFR5	—	10.1 ± 2.5 nM	—	—	4.0 ± 1.5 nM
NFR1	—	4.9 ± 1.3 nM	—	—	0.6 ± 0.25 nM
WGA	25 ± 8 μM	15 ± 3 μM	n/a	n/a	n/a
GFP	—	—	n/a	n/a	n/a

—, not detectable; n/a, not applicable.

The binding affinities we have determined do not distinguish calcium spiking from calcium influx, which in *Lotus* are induced by 0.1–1 nM versus 10 nM Nod factor (15). Binding of Nod factor to the three LysM domains with different affinities might be involved in setting thresholds for these two activation processes but, at present, our methodology is unable to assign the binding directly to any of the LysM domains. More refined studies using, for example, protein concentrations higher than we are able to achieve and maintain in solution, might in the future reveal additional binding sites or affinities contributing to the triggering of the receptors. Elucidation of the binding affinities and possible interactions of the three LysM modules present in the ectodomains of the NFR proteins may be the key to understanding the perception mechanism and remains a challenge for the future.

Materials and Methods

Membrane Purification of NFR1 and NFR5 from *N. benthamiana* and *A. thaliana*. The NFR1 and NFR5 GFP/YFP fusion proteins were extracted from transiently transformed *N. benthamiana* leaves or stably transformed *Arabidopsis*

seedlings grown in liquid culture. Plasma membranes were purified by aqueous two-phase partitioning, and membrane proteins were solubilized with Fos-Choline 10. The GFP_his$_6$ fusion proteins were purified by Ni-NTA affinity chromatography and gel filtration, whereas the YFP_HA fusion proteins were purified by gel filtration. Protein quantification was performed by using in-gel fluorescence against a GFP standard. The yield per gram of tissue was ~20 ng for purifications from the microsomal fraction and 5 ng for purifications from the plasma membrane. Surface plasmon resonance, microscale thermophoresis, and a bead-based assay were used for demonstrating ligand–receptor interactions and determining K_d values. N-terminal sequencing was performed by using automated Edman degradation on a PROCISE sequencer.

Glycan Analysis by MS. Protein bands containing NFR5 expressed in *N. benthamiana* or *A. thaliana* were excised from SDS/PAGE gels, processed, and deglycosylated by using PNGase A. The glycosylated and deglycosylated samples were in-gel digested with trypsin, chymotrypsin, or Asp-N endoproteinase. Samples were then eluted from micro columns onto a target plate, and mass spectra were recorded by using a 4800 *Plus* MALDI TOF/TOF (AB SCIEX) mass spectrometer, operated in reflector, positive ion mode, and acceleration voltage was 20 kV.

Extraction, Purification, and Modification of Ligands. Nod factors were isolated and purified by RP-HPLC using a C18 column. For the labeling, the Nod factor and chitin ligands were coupled to a tetra(ethylene glycol) linker with a reactive aminooxy group in one end and a protected thiol in the other end by oxime coupling, resulting in stable oxime glycoconjugates. The resulting thiol-functionalized conjugates were purified by semipreparative HPLC and linked to Alexa$_{546}$ or immobilized by thiol coupling on CM5 sensor chips.

ACKNOWLEDGMENTS. We thank Svend Dam for suggestions on the processing analysis and Fleur C. Dolman for reading and commenting the manuscript. The Danish National Research Foundation and the European Research Council funded this work.

1. Long SR (1996) Rhizobium symbiosis: Nod factors in perspective. *Plant Cell* 8: 1885–1898.
2. Ehrhardt DW, Atkinson EM, Long SR (1992) Depolarization of alfalfa root hair membrane potential by Rhizobium meliloti Nod factors. *Science* 256:998–1000.
3. Truchet G, et al. (1991) Sulphated lipo-oligosaccharide signals of Rhizobium meliloti elicit root nodule organogenesis in alfalfa. *Nature* 351:670–673.
4. Radutoiu S, et al. (2003) Plant recognition of symbiotic bacteria requires two LysM receptor-like kinases. *Nature* 425:585–592.
5. Madsen EB, et al. (2003) A receptor kinase gene of the LysM type is involved in legume perception of rhizobial signals. *Nature* 425:637–640.
6. Zhukov V, et al. (2008) The pea Sym37 receptor kinase gene controls infection-thread initiation and nodule development. *Mol Plant Microbe Interact* 21:1600–1608.
7. Arrighi JF, et al. (2006) The Medicago truncatula lysin [corrected] motif-receptor-like kinase gene family includes NFP and new nodule-expressed genes. *Plant Physiol* 142: 265–279.
8. Limpens E, et al. (2003) LysM domain receptor kinases regulating rhizobial Nod factor-induced infection. *Science* 302:630–633.
9. Amor BB, et al. (2003) The NFP locus of Medicago truncatula controls an early step of Nod factor signal transduction upstream of a rapid calcium flux and root hair deformation. *Plant J* 34:495–506.
10. Indrasumunar A, et al. (2011) Nodulation factor receptor kinase 1α controls nodule organ number in soybean (Glycine max L. Merr). *Plant J* 65:39–50.
11. Indrasumunar A, et al. (2010) Inactivation of duplicated nod factor receptor 5 (NFR5) genes in recessive loss-of-function non-nodulation mutants of allotetraploid soybean (Glycine max L. Merr.). *Plant Cell Physiol* 51:201–214.
12. Smit P, et al. (2007) Medicago LYK3, an entry receptor in rhizobial nodulation factor signaling. *Plant Physiol* 145:183–191.
13. Felle HH, Kondorosi E, Kondorosi A, Schultze M (2000) How alfalfa root hairs discriminate between Nod factors and oligochitin elicitors. *Plant Physiol* 124:1373–1380.
14. Oldroyd GE, Mitra RM, Wais RJ, Long SR (2001) Evidence for structurally specific negative feedback in the Nod factor signal transduction pathway. *Plant J* 28:191–199.
15. Miwa H, Sun J, Oldroyd GE, Downie JA (2006) Analysis of Nod-factor-induced calcium signaling in root hairs of symbiotically defective mutants of Lotus japonicus. *Mol Plant Microbe Interact* 19:914–923.
16. Walker SA, Viprey V, Downie JA (2000) Dissection of nodulation signaling using pea mutants defective for calcium spiking induced by nod factors and chitin oligomers. *Proc Natl Acad Sci USA* 97:13413–13418.
17. Madsen EB, et al. (2011) Autophosphorylation is essential for the in vivo function of the Lotus japonicus Nod factor receptor 1 and receptor-mediated signalling in cooperation with Nod factor receptor 5. *Plant J* 65:404–417.
18. Klaus-Heisen D, et al. (2011) Structure-function similarities between a plant receptor-like kinase and the human interleukin-1 receptor-associated kinase-4. *J Biol Chem* 286:11202–11210.
19. Haney CH, et al. (2011) Symbiotic rhizobia bacteria trigger a change in localization and dynamics of the Medicago truncatula receptor kinase LYK3. *Plant Cell* 23:2774–2787.
20. Lefebvre B, et al. (2010) A remorin protein interacts with symbiotic receptors and regulates bacterial infection. *Proc Natl Acad Sci USA* 107:2343–2348.
21. Madsen LH, et al. (2010) The molecular network governing nodule organogenesis and infection in the model legume Lotus japonicus. *Nat Commun* 1:10–22.
22. Radutoiu S, et al. (2007) LysM domains mediate lipochitin-oligosaccharide recognition and Nfr genes extend the symbiotic host range. *EMBO J* 26:3923–3935.
23. Bensmihen S, de Billy F, Gough C (2011) Contribution of NFP LysM domains to the recognition of Nod factors during the Medicago truncatula/Sinorhizobium meliloti symbiosis. *PLoS ONE* 6:e26114.
24. Li R, et al. (2011) Natural variation in host-specific nodulation of pea is associated with a haplotype of the SYM37 LysM-type receptor-like kinase. *Mol Plant Microbe Interact* 24:1396–1403.
25. Rothbauer U, et al. (2008) A versatile nanotrap for biochemical and functional studies with fluorescent fusion proteins. *Mol Cell Proteomics* 7:282–289.
26. Thygesen MB, Sauer J, Jensen KJ (2009) Chemoselective capture of glycans for analysis on gold nanoparticles: Carbohydrate oxime tautomers provide functional recognition by proteins. *Chemistry* 15:1649–1660.
27. Thygesen MB, et al. (2010) Nucleophilic catalysis of carbohydrate oxime formation by anilines. *J Org Chem* 75:1752–1755.
28. Lienemann M, et al. (2009) Characterization of the wheat germ agglutinin binding to self-assembled monolayers of neoglycoconjugates by AFM and SPR. *Glycobiology* 19: 633–643.
29. Wienken CJ, Baaske P, Rothbauer U, Braun D, Duhr S (2010) Protein-binding assays in biological liquids using microscale thermophoresis. *Nat Commun* 1:100–107.
30. Hadian K, et al. (2011) NF-κB essential modulator (NEMO) interaction with linear and lys-63 ubiquitin chains contributes to NF-κB activation. *J Biol Chem* 286:26107–26117.
31. Wang X, et al. (2011) Peptide surfactants for cell-free production of functional G protein-coupled receptors. *Proc Natl Acad Sci USA* 108:9049–9054.
32. Mbengue M, et al. (2010) The Medicago truncatula E3 ubiquitin ligase PUB1 interacts with the LYK3 symbiotic receptor and negatively regulates infection and nodulation. *Plant Cell* 22:3474–3488.
33. Liu T, et al. (2012) Chitin-induced dimerization activates a plant immune receptor. *Science* 336:1160–1164.
34. Lefebvre B, et al. (2012) Role of N-glycosylation sites and CXC motifs in trafficking of Medicago trunculata Nod factor perception protein to the plasma membrane. *J Biol Chem* 287:10812–10823.
35. Lerouge P, et al. (1998) N-glycoprotein biosynthesis in plants: Recent developments and future trends. *Plant Mol Biol* 38:31–48.
36. Gomord V, et al. (2010) Plant-specific glycosylation patterns in the context of therapeutic protein production. *Plant Biotechnol J* 8:564–587.
37. Hammond C, Braakman I, Helenius A (1994) Role of N-linked oligosaccharide recognition, glucose trimming, and calnexin in glycoprotein folding and quality control. *Proc Natl Acad Sci USA* 91:913–917.
38. Mulder L, Lefebvre B, Cullimore J, Imberty A (2006) LysM domains of Medicago truncatula NFP protein involved in Nod factor perception. Glycosylation state, molecular modeling and docking of chitooligosaccharides and Nod factors. *Glycobiology* 16:801–809.
39. López-Lara IM, et al. (1995) Structural identification of the lipo-chitin oligosaccharide nodulation signals of Rhizobium loti. *Mol Microbiol* 15:627–638.
40. Bek AS, et al. (2010) Improved characterization of nod factors and genetically based variation in LysM Receptor domains identify amino acids expendable for nod factor recognition in Lotus spp. *Mol Plant Microbe Interact* 23:58–66.
41. Iizasa EI, Mitsutomi M, Nagano Y (2010) Direct binding of a plant LysM receptor-like kinase, LysM RLK1/CERK1, to chitin in vitro. *J Biol Chem* 285:2996–3004.
42. Petutschnig EK, Jones AM, Serazetdinova L, Lipka U, Lipka V (2010) The lysin motif receptor-like kinase (LysM-RLK) CERK1 is a major chitin-binding protein in Arabidopsis thaliana and subject to chitin-induced phosphorylation. *J Biol Chem* 285: 28902–28911.